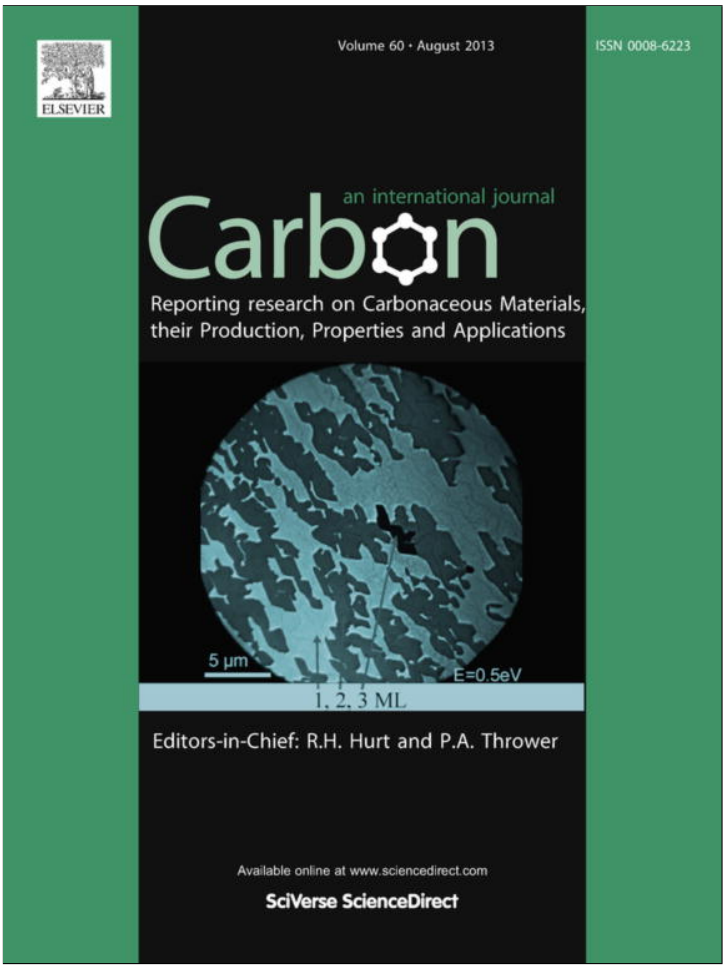

CARBON 60 (2013) 346–355

Available at www.sciencedirect.com

SciVerse ScienceDirect

journal homepage: www.elsevier.com/locate/carbon

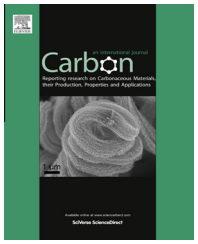

Viscoelastic behavior of carbon black and its relationship with the aggregate size

Shuang Lu [1], *D.D.L. Chung* [*]

Composite Materials Research Laboratory, University at Buffalo, State University of New York, Buffalo, NY 14260-4400, USA

ARTICLE INFO

Article history:
Received 17 January 2013
Accepted 14 April 2013
Available online 19 April 2013

ABSTRACT

The viscoelastic behavior of binderless carbon black compacts under dynamic compression (0.2–10.0 Hz, static strain 1.0–2.5%, deformation amplitude 9.4–16 μm and packing density 0.18–0.45 g/cm^3) is governed by the solid part of the compact, with the elastic character dominating the viscous character. The viscous character increases with increasing aggregate size, while the elastic character decreases. The interparticle movement in an aggregate contributes to the viscous deformation, while the connectivity among the aggregates contributes to the stiffness. The loss tangent of the solid part increases with increasing aggregate size up to 300 nm, which is optimum for viscoelasticity. A larger specific surface area weakly correlates with a lower storage/loss modulus of the solid part. The particle size does not correlate with the viscoelastic behavior. Both viscous and elastic characters increase with increasing static strain, due to the tightening of the solid part. The loss tangent of the solid part is up to 1.2, compared to 21 and 0.67 for exfoliated graphite and rubber respectively. The storage and loss moduli of the solid part (up to 21 and 180 kPa respectively) are below those of rubber, but are above or comparable to those of exfoliated graphite. Possible applications relate to mechanical isolation.

1. Introduction

Carbon black is a carbon material that is in the form of aggregates of nanoparticles [1,2]. It is used in rubber as a reinforcement and in plastics, printing inks, coatings, sealants and other products for pigmentation.

Due to this microstructure and the ease of motion of the particles relative to one another, carbon black is highly compressible (squishable). The squishability enables carbon black to spread in response to an applied compressive force. For example, when carbon black is squeezed between two rigid surfaces, it tends to spread along the interface between the two surfaces.

The spreadability allows carbon black to be an effective additive for enhancing the electrical conductivity of a compact of nonconductive particles in the absence of a matrix. For example, carbon black is commonly mixed with manganese dioxide particles, which are nonconductive and used as an electrode in batteries [3]. The presence of the carbon black renders the electrode conductive, as necessary for battery operation. The high effectiveness of carbon black as a conductive additive stems from the spreadability of carbon black and the consequent ability to form a conductive network. Due to the spreadability, carbon black can be even more effective than carbon nanofiber (originally known as carbon filament) as a conductive additive [3]. In spite of their high

[*] *Corresponding author:* Fax: +1 716 645 2883.
E-mail addresses: hitlu@126.com (S. Lu), ddlchung@buffalo.edu (D.D.L. Chung).
URL: http://alum.mit.edu/www/ddlchung (D.D.L. Chung).
[1] Permanent address: Box 1430, School of Civil Engineering, Harbin Institute of Technology, 66 West Dazhi Street, Nangang District, Harbin 150006, PR China.

0008-6223/$ - see front matter
http://dx.doi.org/10.1016/j.carbon.2013.04.047

aspect ratio, carbon nanofibers and nanotubes are not spreadable.

The squishability also enables carbon black to be conformable to the topography of the surfaces pressed against it. The conformability allows carbon black paste (i.e., a liquid-based paste containing dispersed carbon black) to be highly effective as a thermal paste for the improvement of the thermal contact between two surfaces [4–8]. The conformability also enables carbon black to be effective as an interlaminar filler for improving the through-thickness thermal conductivity of continuous carbon fiber polymer-matrix composites [9].

Carbon black is commonly used as an inexpensive reinforcement in polymer-matrix composites, such as in rubber tires [10–12]. The high effectiveness of carbon black as a reinforcement also relates to the spreadability of carbon black. Although network formation is not necessary for the reinforcing ability, the spreading allows the carbon black to develop a fibrous morphology, which is advantageous for the reinforcing ability.

Carbon black is also used as an electrically conductive filler in polymer-matrix composites for anti-static [13–16] and sensor applications [17,18]. Percolation, which is necessary for the carbon black to enhance the electrical conductivity greatly, relates to the ability for the carbon black to form a network. This ability is enhanced by the squishability of carbon black.

The spreading and conforming mentioned above relate to the rheological behavior (the flow behavior), which pertains to both the elastic and viscous behavior. The elastic aspect relates to mechanical energy storage and the stiffness, as expressed by the storage modulus (i.e., the real part of the complex modulus), whereas the viscous aspect relates to the mechanical energy loss (i.e., the mechanical energy dissipation) and the viscosity, as expressed in terms of the loss tangent (i.e., tan δ, where δ is the phase angle between the stress wave and the strain wave, with $\delta = 0$ for totally elastic behavior and $\delta = 90^\circ$ for totally viscous behavior) and the loss modulus (i.e., the imaginary part of the complex modulus) [19]. Such viscoelastic behavior requires study of the dynamic mechanical properties, because the elastic and viscous types of deformation differ in their time dependence.

In relation to the electrical, thermal and mechanical applications mentioned above, the compressive properties of carbon black are relevant. Although the mechanical properties of polymer-matrix composites containing carbon black have been extensively addressed [20–22], those of carbon black itself have not been previously addressed. Therefore, this paper is primarily directed at studying the dynamic compressive properties of carbon black.

The compressive properties in the plastic deformation regime are relevant to the spreadability and conformability. However, those in the elastic regime are fundamental to understanding the compressive properties in general. Therefore, this paper addresses the dynamic compressive properties of carbon black in the elastic regime, including the effects of the packing density and the static strain on these properties. The packing density relates to the solid volume fraction in the compact and is expected to affect the interaction between adjacent aggregates.

Different types of carbon black tend to be different in the aggregate size. Since the particle–particle interaction within an aggregate differs from the interaction between aggregates, the aggregate size is expected to affect the dynamic compressive properties. A small aggregate size (i.e., carbon black with a lower DBP value or a lower structure) has been reported to help the conformability, due to the lower viscosity and higher spreadability of the resulting paste [8]. Investigation of the effect of the aggregate size on the dynamic compressive properties is the secondary objective of this work.

2. Experimental methods

2.1. Materials

The five types of carbon black used in this work are described in Table 1. They are all furnace blacks, which are made from petroleum feedstocks. In the manufacturing of furnace black, the feedstock being injected into a high-temperature reactor where the hydrocarbon is cracked and dehydrogenated to form carbon with a quasi-graphitic microstructure.

All of the types are fluffy carbon blacks that have not undergone any pelletization process in the manufacturing. They are all supplied by Cabot Corp., Billerica, MA, USA. The true density is 1.8 g/cm^3 and the bulk density ranges from 0.09 to 0.34 g/cm^3. The properties listed in Table 1 include the particle size, the aggregate size, BET specific surface area, DBP (defined below), pH and Φ (the maximum carbon black volume fraction in random media, as defined in Eq. (1) below). The materials studied are in their as-received state.

DBP refers to the dibutyl phthalate absorption number, which is defined as the volume (in ml) of dibutyl phthalate (an oil) that a given mass (100 g) of compressed carbon black can absorb before becoming a paste with a specified viscosity (ASTM D3493-09). The viscosity is mainly governed by the structure of the carbon black, with a higher structure resulting in a higher viscosity, such that the specific surface area has a relatively minor effect on the viscosity. DBP is currently used by the carbon industry as an index for describing the structure of carbon blacks. A low DBP value (such as 32–47, i.e., 32–47 ml/100 g) indicates little particle aggregation or a low structure[2]. A higher DBP value corresponds to a higher structure. Furnace blacks are not in the form of individual spheres of carbon, but are in the form of aggregates of carbon particles that are fused together as grape-like clusters and/or reticulate chains or branches, such that there is a distribution of aggregate sizes. This structure is associated with internal voids. In the DBP determination, oil absorption occurs in these voids. Furnace blacks typically have moderate or high structures with DBP values exceeding 65. The higher the structure, the more is the degree of reticulation. The specific surface area tends to increase with the DBP value, but, for a given DBP value, the specific surface area can take on a wide range of values. This is because the specific surface area increases with decreasing primary particle size. For example,

[2] http://www.cancarb.com/pdf/Physical_Chemical_Properties.pdf.

Table 1 – Characteristics of the five types of carbon black used in this work.

Carbon black type	DBP (ml/100 g)[a]	Average pH[a]	Specific surface area[a] (m^2/g)	Particle size[a] (nm)	Bulk density[a] (g/cm^3)	Φ[b]	Effective aggregate diameter[c] (nm)		Aggregate size range[c] (nm)
							Area-average	Mass-average	
Regal 350R	46	7.7	58	48	0.34	0.547	196	216	35–453
Regal 99R	61–69	8.2	46	38	0.29	0.446–0.476	201	222	54–422
Monarch 570	109–119	8.1	120	21	0.23	0.318–0.338	227	297	24–560
Monarch 280	128–140	7.5	42	45	0.11	0.284–0.302	303	398	31–752
Vulcan XC72R	188	7.5	254	30	0.09	0.228	430	638	36–1122

[a] From manufacturer data sheets.
[b] Relates to DBP and defined and calculated by using Eq. (1).
[c] Measured in this work.

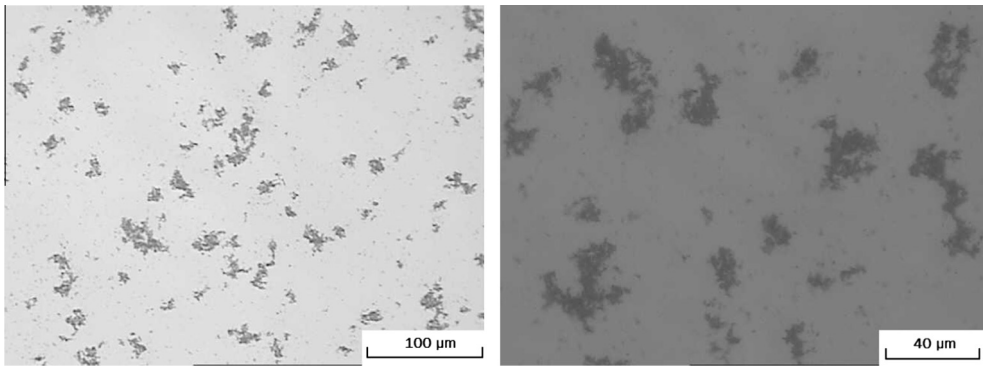

Fig. 1 – Optical microscope images of Vulcan XC72R carbon black. (a) Lower magnification. (b) Higher magnification.

the particle size can be around 8 nm for a carbon black with a high specific surface area and around 75 nm for a carbon black with a low specific surface area[3]. The particle size is the mean primary particle size, as typically measured by transmission electron microscopy.

The different types of carbon black used in this work differ in the combination of DBP value, aggregate size, specific surface area and particle size. As shown in Table 1, Regal 99R has higher DBP, lower specific surface area and smaller particle size than Regal 350R. Monarch 280 has higher DBP, much lower specific surface area, larger aggregate size and larger particle size than Monarch 570. Vulcan XC72R is exceptionally high in the DBP value, aggregate size and specific surface area. The main type of carbon black used in this work is Vulcan XC72R GP-3820; its optical micrographs are shown in Fig. 1.

The aggregate size range and effective aggregate diameter, as measured in this work by laser light scattering (90Plus/BI-MAS, Brookhaven Instruments Corporation, Holtsville, NY) for each type of carbon black, are also shown in Table 1. A higher DBP value correlates with a larger effective diameter, as expected.

The carbon black structure is related to the maximum packing fraction, which is defined as the maximum fraction of particles in a given matrix. Thus, the DBP value allows one to calculate the maximum carbon black volume fraction (Φ) in random media according to the relation [23].

$$\Phi = (1 + \rho D)^{-1}, \quad (1)$$

where ρ is the density of the carbon black and D is the DBP value. A higher DBP value gives a higher value of Φ. The value of Φ is related to the yield stress of the carbon black suspension [24]. The values of Φ, as calculated by using Eq. (1), are listed in Table 1.

2.2. *Testing methods*

Specimens are obtained by manual compaction in a stainless steel cylindrical cup of inside diameter 18.0 mm (Fig. 2). The thickness of the specimen in the direction of the compressive stress (the vertical direction in Fig. 2) is 3.5 mm, as measured for each specimen. The packing density is obtained from the measured mass and the measured volume, which relates to the thickness. Specimens are tested at packing densities ranging from 0.18 to 0.45 g/cm^3. With the true density of carbon black at 1.8 g/cm^3, these untreated compact density values correspond to solid volume fractions ranging from 10% to 25%. Dynamic compressive stress is applied by using a stainless steel circular plate of diameter 15.0 mm, such that the plate is parallel to the bottom plane of the cup and is cen-

[3] http://www.cabot-corp.com/Specialty-Carbon-Blacks/KBase?recOffset=20.

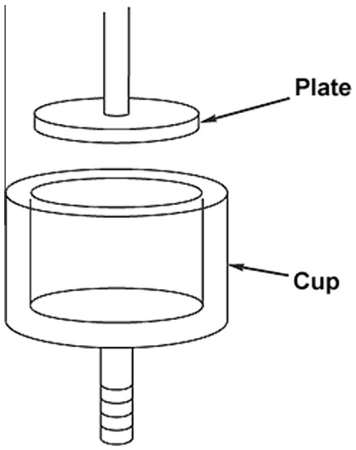

Fig. 2 – Cup-and-plate specimen holder for dynamic compressive testing. The plate has diameter 15 mm; the cup has inside diameter 18 mm. The holder is an accessory of the dynamic mechanical analyzer.

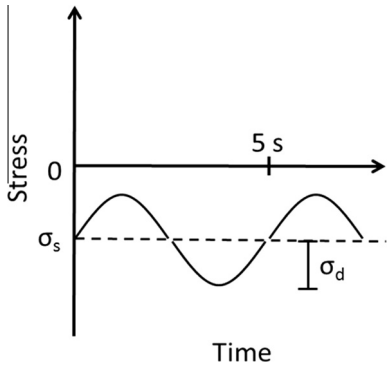

Fig. 3 – Schematic illustrations of the variation of the stress with time during dynamic mechanical compression at 0.2 Hz. The static and dynamic stresses are σ_s and σ_d respectively.

tered at the axis of the cup. Three specimens are tested for each combination of specimen type and loading condition.

Dynamic compressive testing (ASTM D 4065-12[4]) using a sinusoidal stress wave at controlled frequencies of 0.2–10.0 Hz is conducted at room temperature using a dynamic mechanical analyzer (DMA7E, Perkin Elmer Corp., Shelton, CT). The cyclic variation of stress with time is illustrated in Fig. 3 for 0.2 Hz. The phase lag between the input stress wave and the output strain wave is measured, thus giving tan δ. The amplitude of the stress wave (as controlled by a load cell) divided by the amplitude of the strain wave (as measured by a displacement transducer) gives the storage modulus. The product of the storage modulus and the tan δ gives the loss modulus. The dynamic stress σ_d ranges from 67% to 86% of the corresponding static stress σ_s. The stresses are chosen so that different specimens are tested at comparable values of the static strain and deformation amplitude, unless the static strain is intentionally varied in order to study its effect. The static stress ranges from 80 to 1100 Pa, the dynamic stress ranges from 60 to 900 Pa, and the static strain ranges from 0.98% to 2.64%. Similar values of the static strain are obtained by adjusting the static stress and dynamic stress, such that the deformation amplitude is kept below 16 μm in order to avoid the presence of multiple vibration modes, The frequency is far from any vibration resonance frequency.

3. Results and discussion

3.1. *Effects of the packing density, static strain and frequency*

Tables 2 and 3 show the dynamic compressive properties of Vulcan XC72R carbon black. As shown in Table 2, the loss tangent, storage modulus and loss modulus of the compact all increase with increasing static strain and with increasing packing density, though the increase in the loss tangent is slight. Both an increase in the packing density and an increase in the static strain are associated with a higher degree of compaction. The increase in loss tangent indicates that enhanced interaction between the aggregates, as enabled by the increased degree of compaction, increases the viscous character. The increase in storage modulus indicates that the enhanced interaction between the aggregates also increases the stiffness. Hence, the highest values of the loss tangent, storage modulus and loss modulus are obtained for the combination of highest packing density and highest static strain.

Table 2 shows the ratio of the storage modulus to the solid content (i.e., the solid volume fraction), which, based on the Rule of Mixtures, is equal to the storage modulus of the solid part of the compact, since the air in the compact does not contribute to the stiffness. Table 2 also shows the ratio of the loss modulus to the solid content, which, based on the Rule of Mixtures, is equal to the loss modulus of the solid part of the compact.

The loss tangent divided by the solid content relates to the loss tangent of the solid part of the compact, as based on the Rule of Mixtures. The Rule of Mixtures for the loss tangent [25] is less established than that for the storage or loss modulus. However, its validity is supported by the notion that the air in the carbon black compact essentially does not contribute to the viscous deformation. The loss tangent divided by the solid content shows correlation with the aggregate size, specific surface area and the particle size, as shown below, but the loss tangent itself shows no correlation with these quantities.

As shown in Table 2, the storage/loss modulus divided by the solid content is essentially independent of the packing density when the static strain is below 2% (i.e., the first two columns of data in Table 2), though it increases moderately with increasing packing density when the static strain exceeds 2% (i.e., the last two columns of data in Table 2). The loss tangent divided by the solid content decreases slightly with increasing packing density for static strains both below and above 2%. The weak effect of the packing density on the loss tangent divided by the solid content is also indicated by Fig. 4. The weak effect of the packing density on the moduli

[4] ASTM D4065 – 12, "Standard Practice for Plastics: Dynamic Mechanical Properties: Determination and Report of Procedures". This method is commonly used for obtaining dynamic mechanical data.

Table 2 – Effects of the packing density and the static strain on the dynamic compressive properties of carbon black (Cabot Vulcan XC72R) compacts at the frequency of 0.2 Hz.

Density (g/cm^3)	Solid content (vol.%)	Dynamic compressive properties				
0.18 ± 0.01	**10 ± 1**	Static stress (Pa)	120	140	160	200
		Dynamic stress (Pa)	80	120	120	160
		Static strain (%)	1.09 ± 0.12	1.85 ± 0.11	2.21 ± 0.08	2.53 ± 0.12
		Amplitude (μm)	12.3	12.9	13.7	14.9
		Loss tangent	**0.092 ± 0.004**	**0.110 ± 0.011**	**0.114 ± 0.005**	**0.120 ± 0.002**
		Storage modulus (10^3 Pa)	**1.37 ± 0.23**	**2.24 ± 0.14**	**2.38 ± 0.14**	**2.57 ± 0.12**
		Loss modulus (10^2 Pa)	**1.26 ± 0.16**	**2.46 ± 0.10**	**2.71 ± 0.05**	**3.08 ± 0.13**
		Loss tangent/solid content	*0.93 ± 0.13*	*1.12 ± 0.31*	*1.15 ± 0.23*	*1.21 ± 0.20*
		Storage modulus/solid content (10^3 Pa)	*14 ± 4*	*23 ± 4*	*24 ± 4*	*26 ± 4*
		Loss modulus/solid content (10^2 Pa)	*13 ± 3*	*25 ± 3*	*24 ± 1*	*32 ± 4*
0.23 ± 0.01	**13 ± 1**	Static stress (Pa)	140	160	200	240
		Dynamic stress (Pa)	120	140	160	200
		Static strain (%)	1.38 ± 0.08	1.79 ± 0.09	2.03 ± 0.10	2.39 ± 0.13
		Amplitude (μm)	11.5	13.3	14.0	15.2
		Loss tangent	**0.108 ± 0.013**	**0.110 ± 0.003**	**0.117 ± 0.002**	**0.123 ± 0.006**
		Storage modulus (10^3 Pa)	**1.67 ± 0.15**	**2.61 ± 0.10**	**3.88 ± 0.09**	**4.11 ± 0.13**
		Loss modulus (10^2 Pa)	**1.79 ± 0.06**	**2.87 ± 0.05**	**4.54 ± 0.05**	**5.05 ± 0.11**
		Loss tangent/solid content	*0.80 ± 0.17*	*0.85 ± 0.13*	*0.91 ± 0.12*	*0.96 ± 0.17*
		Storage modulus/solid content (10^3 Pa)	*13 ± 2*	*21 ± 3*	*30 ± 3*	*31 ± 4*
		Loss modulus/solid content (10^2 Pa)	*13 ± 2*	*22 ± 2*	*35 ± 3*	*39 ± 4*
0.27 ± 0.01	**15 ± 1**	Static stress (Pa)	150	200	300	350
		Dynamic stress (Pa)	100	150	200	250
		Static strain (%)	1.12 ± 0.09	1.66 ± 0.12	2.15 ± 0.17	2.64 ± 0.13
		Amplitude (μm)	11.2	13.3	14.8	15.7
		Loss tangent	**0.109 ± 0.005**	**0.112 ± 0.002**	**0.124 ± 0.004**	**0.129 ± 0.002**
		Storage modulus (10^3 Pa)	**1.94 ± 0.06**	**3.24 ± 0.09**	**5.51 ± 0.11**	**6.54 ± 0.11**
		Loss modulus (10^2 Pa)	**2.11 ± 0.03**	**3.63 ± 0.05**	**6.83 ± 0.06**	**8.44 ± 0.10**
		Loss tangent/solid content	*0.73 ± 0.12*	*0.75 ± 0.09*	*0.83 ± 0.12*	*0.86 ± 0.10*
		Storage modulus/solid content (10^3 Pa)	*13 ± 1*	*22 ± 2*	*37 ± 3*	*44 ± 4*
		Loss modulus/solid content (10^2 Pa)	*14 ± 1*	*24 ± 2*	*46 ± 3*	*56 ± 5*
0.31 ± 0.01	**17 ± 1**	Static stress (Pa)	200	250	320	360
		Dynamic stress (Pa)	150	200	240	280
		Static strain (%)	1.51 ± 0.09	1.86 ± 0.11	2.23 ± 0.15	2.53 ± 0.13
		Amplitude (μm)	12.3	14.6	15.3	16.1
		Loss tangent	**0.116 ± 0.001**	**0.125 ± 0.003**	**0.133 ± 0.001**	**0.138 ± 0.004**
		Storage modulus (10^3 Pa)	**2.51 ± 0.07**	**3.62 ± 0.11**	**5.83 ± 0.10**	**6.79 ± 0.12**
		Loss modulus (10^2 Pa)	**2.91 ± 0.05**	**4.52 ± 0.05**	**7.75 ± 0.06**	**9.37 ± 0.12**
		Loss tangent/solid content	*0.69 ± 0.07*	*0.74 ± 0.09*	*0.79 ± 0.07*	*0.82 ± 0.10*
		Storage modulus/solid content (10^3 Pa)	*15 ± 1*	*21 ± 2*	*35 ± 3*	*40 ± 3*
		Loss modulus/solid content (10^2 Pa)	*17 ± 2*	*26 ± 2*	*46 ± 3*	*55 ± 4*

Table 3 – Effects of the frequency and the static strain on the dynamic compressive properties of carbon black (Cabot Vulcan XC72R) compact of packing density 0.27 g/cm^3.

Frequency (Hz)	Dynamic compressive properties			
	Static stress (Pa)	150	200	300
	Dynamic stress (Pa)	100	150	200
0.2	Static strain (%)	1.12 ± 0.09	1.66 ± 0.12	2.15 ± 0.17
	Deformation amplitude (μm)	11.2	13.3	14.8
	Loss tangent	**0.109 ± 0.005**	**0.112 ± 0.002**	**0.124 ± 0.002**
	Storage modulus (10^3 Pa)	**1.94 ± 0.06**	**3.24 ± 0.09**	**5.51 ± 0.11**
	Loss modulus (10^2 Pa)	**2.11 ± 0.03**	**3.63 ± 0.05**	**6.83 ± 0.06**
1.0	Static strain (%)	1.04 ± 0.06	1.55 ± 0.12	2.13 ± 0.13
	Amplitude (μm)	12.5	14.1	15.0
	Loss tangent	**0.097 ± 0.006**	**0.109 ± 0.002**	**0.119 ± 0.002**
	Storage modulus (10^3 Pa)	**1.87 ± 0.08**	**3.11 ± 0.12**	**4.86 ± 0.09**
	Loss modulus (10^2 Pa)	**1.81 ± 0.04**	**3.39 ± 0.08**	**5.78 ± 0.09**
5.0	Static strain (%)	0.99 ± 0.08	1.46 ± 0.05	1.93 ± 0.09
	Amplitude (μm)	13.7	14.5	15.4
	Loss tangent	**0.075 ± 0.004**	**0.081 ± 0.002**	**0.082 ± 0.003**
	Storage modulus (10^3 Pa)	**1.64 ± 0.11**	**2.83 ± 0.15**	**4.38 ± 0.08**
	Loss modulus (10^2 Pa)	**1.23 ± 0.10**	**2.29 ± 0.18**	**3.59 ± 0.13**
10.0	Static strain (%)	0.98 ± 0.12	1.31 ± 0.10	1.59 ± 0.09
	Amplitude (μm)	14.1	14.8	15.7
	Loss tangent	**0.053 ± 0.008**	**0.061 ± 0.002**	**0.066 ± 0.004**
	Storage modulus (10^3 Pa)	**1.59 ± 0.09**	**2.75 ± 0.09**	**3.75 ± 0.13**
	Loss modulus (10^2 Pa)	**0.84 ± 0.11**	**1.67 ± 0.09**	**2.48 ± 0.15**

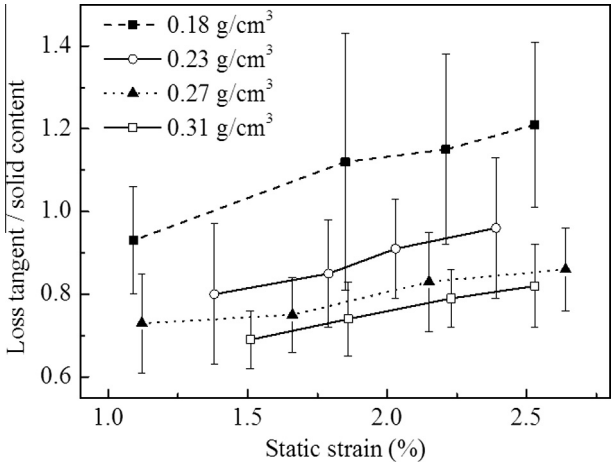

Fig. 4 – Effect of the static strain on the loss tangent/solid content based on the data in Table 2.

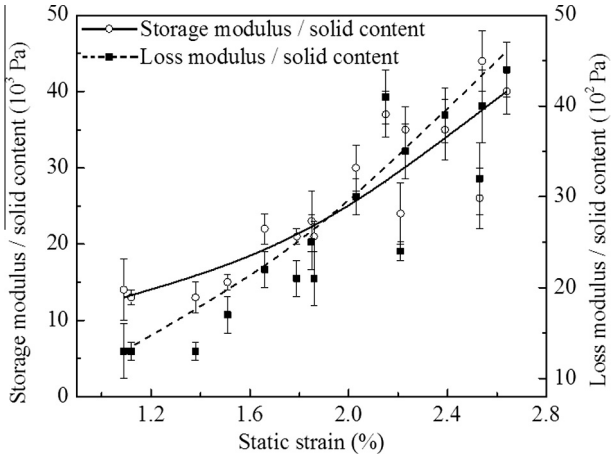

Fig. 5 – Effect of the static strain on the storage modulus/solid content and on the loss modulus/solid content based on the data in Table 2.

and loss tangent, both divided by the solid content, indicates that both the elastic and viscous characters of the compact are mainly governed by the solid part of the compact. In other words, the deformation within the solid part, as enabled by the microstructure of the solid part, mainly governs the viscoelastic behavior of the compact.

Fig. 4 shows that the loss tangent divided by the solid content increases with increasing static strain for each value of the solid content, as obtained from the data in Table 2 for Vulcan XC72R. The fact that the curves for the different solid contents do not overlap is consistent with the notion that the simple Rule of Mixtures does not apply well to the loss tangent. Nevertheless, Fig. 4 shows that a higher static strain enhances the viscous character, whereas a higher solid content (i.e., a higher packing density) decreases the viscous character. Since both a higher static strain and a higher solid content correspond to a higher degree of compaction, the two treads appear to be contradictory. The apparent contradiction suggests that the viscous deformation is sensitive to the degree of compaction, such that the relationship between these two quantities is not simple.

Also based on the data for Vulcan XC72R carbon black in Table 2, Fig. 5 shows that the storage/loss modulus divided by the solid content increases with increasing static strain, such that the curves for the different solid contents essen-

Table 4 – Dynamic compressive properties of carbon black compacts at 0.2 Hz. All data are obtained at comparable values of the static strain and amplitude.

Attribute	REGAL 350R	REGAL 99R	Monarch 570	Monarch 280	Vulcan XC72R	Exfoliated graphite [19]
Density (g/cm^3)	0.44 ± 0.01	0.45 ± 0.01	0.34 ± 0.01	0.25 ± 0.01	0.18 ± 0.01	0.0267
Solid content (vol.%)	24 ± 1	25 ± 1	19 ± 1	17 ± 1	10 ± 1	1.2[d]
Static stress (Pa)	1100	1000	800	550	160	400
Dynamic stress (Pa)	900	700	600	400	120	200
Static strain (%)	2.36 ± 0.12	2.47 ± 0.10	2.23 ± 0.12	2.31 ± 0.09	2.21 ± 0.08	2.0%
Amplitude (μm)	10.2	10.1	10.5	10.3	13.7	6
Loss tangent	**0.117 ± 0.004**	**0.137 ± 0.006**	**0.141 ± 0.008**	**0.207 ± 0.005**	**0.114 ± 0.005**	**0.256**
Storage modulus (kPa)	**42.1 ± 0.7**	**29.6 ± 1.0**	**25.3 ± 0.9**	**12.3 ± 0.8**	**2.38 ± 0.14**	**0.4**
Loss modulus (kPa)	**4.92 ± 0.08**	**4.05 ± 0.12**	**3.56 ± 0.08**	**2.54 ± 0.11**	**0.27 ± 0.01**	**0.1**
***Loss tangent/solid content*[a]**	*0.49 ± 0.05*	*0.55 ± 0.07*	*0.75 ± 0.12*	*1.22 ± 0.14*	*1.16 ± 0.23*	*21*
Storage modulus/solid content*[b] *(kPa)	*176 ± 10*	*119 ± 9*	*134 ± 12*	*61 ± 8*	*24 ± 4*	*33*
Loss modulus/solid content*[c] *(kPa)	*21 ± 1*	*16 ± 1*	*19 ± 2*	*9 ± 2*	*2 ± 1*	*8.3*

[a] Corresponding to the loss tangent of the solid part of the compact, as based on the Rule of Mixtures.
[b] Corresponding to the storage modulus of the solid part of the compact, as based on the Rule of Mixtures.
[c] Corresponding to the loss modulus of the solid part of the compact, as based on the Rule of Mixtures.
[d] Calculated as the density of the exfoliated graphite compact divided by the density of 2.26 g/cm^3 for graphite.

tially overlap. The essential overlap supports the validity of the Rule of Mixtures for the moduli. The fact that the moduli divided by the solid content increase with increasing static strain means that the solid part tightens with increasing static strain. The combination of Figs. 4 and 5 indicates that the loss tangent, storage modulus and loss modulus, each divided by the solid content, all increase with increasing static strain. This means that both the viscous and elastic characters increase with increasing static strain. In other words, the tightening of the solid part enhances both the stiffness and the viscous character.

Table 3 shows that an increase in frequency from 0.2 to 10.0 Hz results in decreases in the loss tangent, storage modulus and loss modulus. The trend is the same for any of the static strain values, but the fractional decrease in the loss tangent is greater than the fractional decrease in the storage modulus. This means that the viscous character is more sensitive to the frequency than the elastic character. This is expected, due to the time required for viscoelastic deformation to occur and the association of the loss tangent to the viscous character. The higher the frequency, the less is the time available for the deformation to occur.

3.2. *Comparison of various carbon blacks*

Table 4 shows comparative data for the dynamic compressive properties of various types of carbon black. The relationships between the various quantities are further depicted in Figs. 6–8, as discussed below.

Fig. 6 shows that the loss tangent divided by the solid content increases with increasing area-average aggregate size up to 300 nm. The trend is the same for the mass-average aggregate size (not shown). This means that an increase in the aggregate size enhances the viscous character and that the interparticle movement in an aggregate contributes significantly to the viscous deformation. If the interaggregate move-

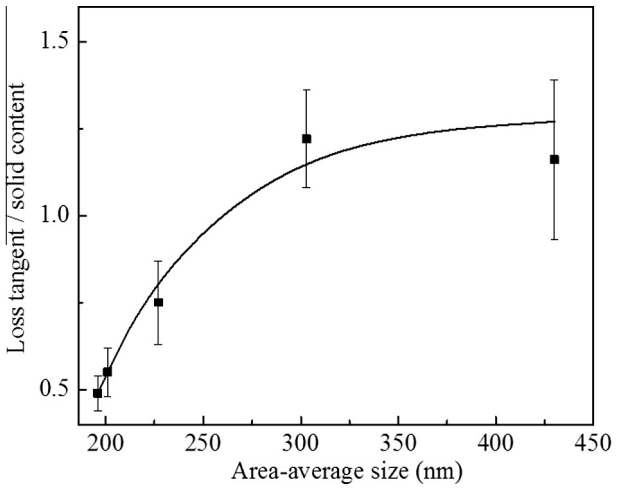

Fig. 6 – Correlation of the average aggregate size with the loss tangent/solid content. The frequency is 0.2 Hz. The data include those for all five types of carbon black studied.

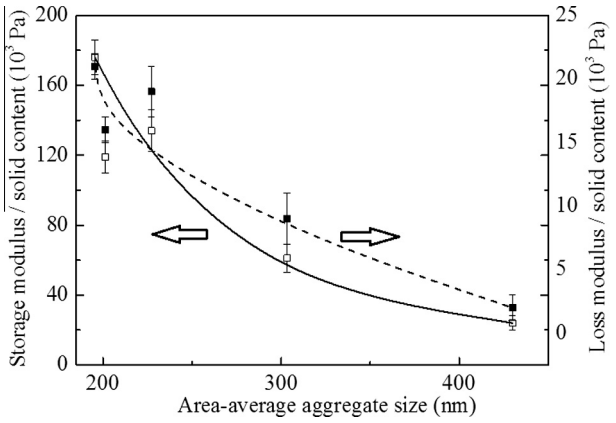

Fig. 7 – Correlation of the average aggregate size with the storage modulus/solid content and with the loss modulus/solid content. The frequency is 0.2 Hz. The data include those for all five types of carbon black studied. Solid squares: loss modulus/solid content. Open squares: storage modulus/solid content.

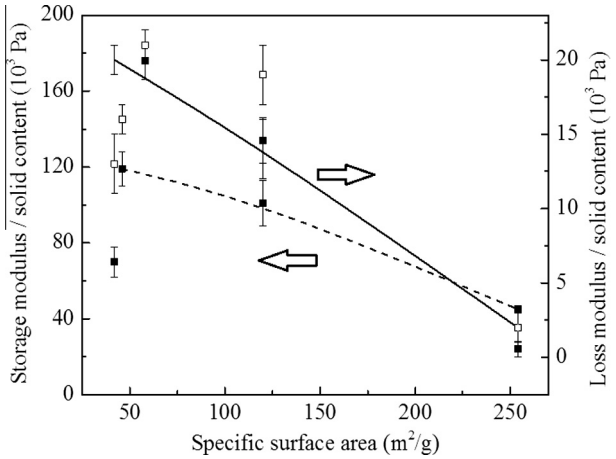

Fig. 8 – A degree of correlation of the specific surface area with the storage modulus/solid content and with the loss modulus/solid content. The frequency is 0.2 Hz. The data include those for all five types of carbon black studied. Solid square: storage modulus/solid content. Open square: loss modulus/solid content.

ment is dominant in providing the viscous character, the loss tangent divided by the solid content would, instead, decrease with increasing aggregate size. However, the loss tangent divided by the solid content exhibits no correlation with the specific surface area or the particle size.

The correlation of the area-average aggregate size with the storage/loss modulus divided by the solid content is shown in Fig. 7. The plot is similar for the mass-average aggregate size (not shown). The correlation is such that the greater is the aggregate size, the lower is the storage/loss modulus divided by the solid content. This means that a larger aggregate size is associated with lower stiffness of the solid part, due to decreased connectivity between adjacent aggregates. In other words, an increase in the aggregate size weakens the interface between the aggregates in the compact. The decreased connectivity is separately supported by visual examination of the compact.

Also based on the data for the five types of carbon black, Fig. 8 shows that a larger value of the specific surface area correlates to a limited degree with a lower value of the storage/loss modulus divided by the solid content. However, the degree of correlation is not as strong as that for the aggregate size (Fig. 7). Fig. 8 suggests that the coherence among the aggregates is diminished by a large surface area, probably due to the functional groups on the surface of the carbon. There is no correlation between the particle size and the storage/loss modulus divided by the solid content.

Comparison of the compacts of the Monarch 570 carbon black at two different packing densities in Table 5 shows that the storage modulus of the compact increases with increasing solid content, while that of the solid part of the compact is essentially independent of the solid content, as expected. Comparison in terms of the loss tangent shows that the loss tangent increases with increasing solid content, while that of the solid part is essentially independent of the solid content. Comparison in terms of the loss modulus shows that the loss modulus of the compact increases with increasing solid content, while that of the solid part is independent of the solid content. These results mean that both the elastic character and the viscous character of the compact are governed by the solid part of the compact. This effect of the packing density for Monarch 570 is consistent with that for Vulcan XC72R (Table 2).

The loss tangent, storage modulus and loss modulus of the compact, and the storage modulus and loss modulus of the solid part (i.e., these quantities divided by the solid content) all decrease with increasing frequencies up to 10.0 Hz (the highest frequency investigated) for any of the five types of carbon black studied. The values for the five types of carbon black relative to one another are similar in Table 4 (0.2 Hz) and Table 6 (5.0 Hz).

At 0.2 Hz, the loss tangent divided by the solid content ranges from 0.5 to 1.2 (with the loss tangent of the compact ranging from 0.11 to 0.21), the storage modulus divided by the solid content ranges from 24 to 180 kPa (with the storage modulus of the compact ranging from 2.4 to 42 kPa), and the loss modulus divided by the solid content ranges from 2 to

Table 5 – Effect of the packing density on the dynamic compressive properties of Monarch 570 carbon black compacts at 0.2 Hz. Data are obtained at comparable values of the static strain and amplitude.

Attribute	Monarch 570	
Density (g/cm^3)	0.34 ± 0.01	0.41 ± 0.01
Solid content (vol.%)	19 ± 1	23 ± 1
Static stress (Pa)	700	800
Dynamic stress (Pa)	500	600
Static strain (%)	1.93 ± 0.13	1.96 ± 0.13
Amplitude (μm)	9.6	9.5
Loss tangent	**0.133 ± 0.007**	**0.149 ± 0.005**
Storage modulus (10^3 Pa)	**19.3 ± 0.9**	**21.7 ± 0.9**
Loss modulus (10^3 Pa)	**2.56 ± 0.09**	**3.17 ± 0.15**
***Loss tangent/solid content*[a]**	**0.70 ± 0.10**	**0.65 ± 0.07**
***Storage modulus/solid content*[b] (10^3 Pa)**	**102 ± 10**	**95 ± 8**
***Loss modulus/solid content*[c] (10^3 Pa)**	**14 ± 2**	**14 ± 1**

[a] Corresponding to the loss tangent of the solid part of the compact, as based on the Rule of Mixtures.
[b] Corresponding to the storage modulus of the solid part of the compact, as based on the Rule of Mixtures.
[c] Corresponding to the loss modulus of the solid part of the compact, as based on the Rule of Mixtures.

Table 6 – Dynamic compressive properties of carbon black compacts at 5.0 Hz. All data are obtained at comparable values of the static strain and amplitude.

Attribute	Regal 350R	Regal 99R	Monarch 570	Monarch 280	Vulcan XC72R
Density (g/cm^3)	0.44 ± 0.01	0.45 ± 0.01	0.34 ± 0.01	0.31 ± 0.01	0.23 ± 0.01
Solid content (vol.%)	24 ± 1	25 ± 1	19 ± 1	17 ± 1	13 ± 1
Static stress (Pa)	1000	900	800	600	200
Dynamic stress (Pa)	800	700	600	450	160
Static strain (%)	1.90 ± 0.12	1.95 ± 0.16	1.97 ± 0.15	1.92 ± 0.12	1.94 ± 0.12
Amplitude (μm)	9.5	9.4	9.7	10.1	12.7
Loss tangent	**0.075 ± 0.004**	**0.120 ± 0.002**	**0.112 ± 0.007**	**0.157 ± 0.024**	**0.093 ± 0.005**
Storage modulus (10^3 Pa)	**34.5 ± 0.7**	**21.3 ± 0.6**	**18.3 ± 1.2**	**10.2 ± 0.9**	**3.53 ± 0.10**
Loss modulus (10^3 Pa)	**2.59 ± 0.09**	**2.56 ± 0.07**	**2.05 ± 0.12**	**1.59 ± 0.14**	**0.33 ± 0.01**
Loss tangent/solid content[a]	*0.31 ± 0.04*	*0.48 ± 0.04*	*0.59 ± 0.10*	*0.94 ± 0.28*	*0.72 ± 0.13*
Storage modulus/solid content[b] *(10^3 Pa)*	*144 ± 9*	*85 ± 6*	*97 ± 11*	*61 ± 8*	*27 ± 3*
Loss modulus/solid content[c] *(10^3 Pa)*	*11 ± 1*	*10 ± 1*	*11 ± 1*	*9 ± 2*	*1 ± 1*

[a] Corresponding to the loss tangent of the solid part of the compact, as based on the Rule of Mixtures.
[b] Corresponding to the storage modulus of the solid part of the compact, as based on the Rule of Mixtures.
[c] Corresponding to the loss modulus of the solid part of the compact, as based on the Rule of Mixtures.

21 kPa (with the loss modulus of the compact ranging from 0.27 to 4.9 kPa). That the storage modulus is much higher than the loss modulus indicates the dominance of elastic character over the viscous character. Nevertheless, the loss tangent is quite high, with the values for the compact (up to 0.21) being comparable to the values for monolithic polymers [26] and the values for the solid part (up to 1.2) being comparable to or higher than that of rubber (0.67) [26]. On the other hand, the storage and loss moduli of the solid part are much lower than those of monolithic polymers [26]. The low values of the moduli mean that the carbon black compact is not effective for mechanical energy dissipation. However, the high values of the loss tangent mean that the carbon black compact is effective for mechanical isolation, i.e., mechanically isolating two objects so that the mechanical energy from one object is not transmitted to the other object. Rubber is typically used for mechanical isolation, but it suffers from the tendency to degrade under the ultraviolet radiation from the sun and from the inability to withstand elevated temperatures. In contrast, carbon is chemically and thermally much more stable than rubber and polymers. Possible applications of carbon black compacts for mechanical isolation relate to filters, fluidized beds, packings and microelectromechanical systems.

For vibration damping and mechanical isolation applications, the most attractive type of carbon black among the five types studied here is Monarch 280, due to its combination of high loss tangent and high loss modulus. This combination of properties results from the optimum aggregate size (area-average aggregate size = 303 nm), as an increase in aggregate size increases the loss tangent (Fig. 6) but decreases the loss modulus (Fig. 7).

The dynamic compressive properties of flexible graphite made by compressing exfoliated graphite [19] and tested using the same frequency (0.2 Hz), static strain (2%), method and equipment as this work are shown in Table 4 for the sake of comparison with the corresponding properties of carbon black. The loss tangent of exfoliated graphite (0.26) is higher than that of any of the five types of carbon black. Due to the low solid content of the exfoliated graphite, the loss tangent divided by the solid content is very high (21) compared to those of carbon black. The storage modulus of exfoliated graphite (0.4 kPa) is lower than those of any of the five types of carbon black, while the storage modulus divided by the solid content (33 kPa) is lower than most of the five types of carbon black. The loss modulus of exfoliated graphite (0.1 kPa) is lower than those of any of the five types of carbon black, while the loss modulus divided by the solid content (8.3 kPa) is lower than those of Regal 350R, Regal 99R and Monarch 570. This means that the exfoliated graphite is superior to all five types of carbon black for mechanical isolation, but is comparable or inferior to the carbon black in terms of the moduli. The high loss tangent of exfoliated graphite is attributed to (i) the layered structure inside the wall of the cells of exfoliated graphite, (ii) the large area of the interface between the layers, and (iii) the fact that the sliding of the layers relative to one another provides a mechanism for viscous deformation. In contrast, carbon black has a particulate structure. The area of the interface between the carbon black particles is small compared the interface area in exfoliated graphite. On the other hand, the storage/loss modulus divided by the solid content is not high for exfoliated graphite, due to the easy shear between the carbon layers.

4. Conclusion

A carbon black compact is viscoelastic. Both the elastic and viscous characters are governed by the solid part of the compact. The elastic character dominates the viscous character. The storage and loss moduli of the solid part are lower than those of rubber, but are higher than or comparable to those of exfoliated graphite. The loss tangent of the solid part is up to 1.2, compared to 21 for exfoliated graphite [19] and 0.67 for rubber [26].

The viscous character increases with increasing aggregate size while the elastic character decreases with increasing aggregate size. The interparticle movement in an aggregate contributes significantly to the viscous deformation, while the connectivity between the aggregates contributes to the stiffness. The loss tangent of the solid part increases with

increasing aggregate size up to 300 nm. However, a greater aggregate size is associated with lower stiffness of the solid part, thus resulting in lower storage and loss moduli of the solid part. For high values of both the loss tangent and the loss modulus, an aggregate size of 300 nm is optimum. A larger specific surface area weakly correlates with a lower storage/loss modulus of the solid part. The particle size does not correlate with the loss tangent or the moduli of the solid part.

Both the viscous and elastic characters increase with increasing static strain, due to the tightening of the solid part, as shown by increases in the loss tangent, storage modulus and loss modulus of the solid part. An increase in frequency decreases the loss tangent, storage modulus and loss modulus. The viscous character is more sensitive to the frequency than the elastic character.

REFERENCES

[1] Gerspacher M. Carbon black characterization – aggregates part 1. KGK, Kautsch Gummi Kunstst 2006;59(11):609–13.

[2] Donet J, Bansal RC, Wang M. Carbon black. 2nd ed. New York, NY: Marcel Dekker; 1993.

[3] Frysz CA, Xiaoping S, Chung DDL. Carbon filaments and carbon black as a conductive additive to the manganese dioxide cathode of a lithium electrolytic cell. J Power Sources 1996;58(1):41–54.

[4] Chia-Ken Leong C, Chung DDL. Carbon black dispersions and carbon-silver combinations as thermal pastes that surpass commercial silver and ceramic pastes in providing high thermal contact conductance. Carbon 2004;42(11):2323–7.

[5] Leong C, Aoyagi Y, Chung DDL. Carbon black pastes as coatings for improving thermal gap-filling materials. Carbon 2006;44(3):435–40.

[6] Lin C, Chung DDL. Graphite nanopletelet pastes versus carbon black pastes as thermal interface materials. Carbon 2009;47(1):295–305.

[7] Hu K, Chung DDL. Flexible graphite modified by carbon black paste for use as a thermal interface material. Carbon 2011;49:1075–86.

[8] Lin C, Chung DDL. Effect of carbon black structure on the effectiveness of carbon black thermal interface pastes. Carbon 2007;45(15):2922–31.

[9] Han H, Lin JT, Aoyagi Y, Chung DDL. Enhancing the thermal conductivity and compressive modulus of carbon fiber polymer-matrix composites in the through-thickness direction by nanostructuring the interlaminar interface with carbon black. Carbon 2008;46(7):1060–71.

[10] Mostafa A, Abouel-Kasem A, Bayoumi MR, El-Sebaie MG. Rubber–filler interactions and its effect in rheological and mechanical properties of filled compounds. J Test Eval 2010;38(3):347–59.

[11] Gerspacher M, O'Farrell CP. Carbon black-elastomer composites. Educ Symp – Am Chem Soc, Rubber Div 2002;49(Chemistry and Physics of Network Formation):E1–E13.

[12] Gerspacher M, Advanced CB. Characterizations to better understand polymer-filler interaction. A critical survey. KGK, Kautsch Gummi Kunstst 2009;62(5).

[13] Polet R. Permanent antistatic compounds for monofilaments and tapes. Chem Fibers Int 2004;54(4):252–3.

[14] Huang J. Carbon black filled conducting polymers and polymer blends. Adv Polym Technol 2002;21(4):299–313.

[15] Carmona F, Ravier J. Electrical properties and meso-structure of carbon black-filled polymers. Carbon 2002;40(2):151–6.

[16] Probst N, Van Bellingen C, Van den Bergh H. Compounding with conductive carbon black. Plast Addit Compounding 2009;11(3):24–7.

[17] El Hasnaoui M, Graca MPF, Achour ME, Costa LC, Outzourhit A, Oueriagli A, et al. Effect of temperature on the electrical properties of copolymer/carbon black mixtures. J Non-Cryst Solids 2010;356(31–32):1536–41.

[18] Loffredo F, De Girolamo Del Mauro A, Burrasca G, La Ferrara V, Quercia L, Massera E, Di Francia G, Della Sala D. Ink-jet printing technique in polymer/carbon black sensing device fabrication. Sens Actuators, B 2009;B143(1):421–9.

[19] Chen P, Chung DDL. Dynamic mechanical properties of flexible graphite made from exfoliated graphite. Carbon 2012;50:283–9.

[20] Hassan MA, Abouel-Kasem A, El-Sharief MA, Yusof F. Evaluation of the material constants of nitrile butadiene rubbers (NBRs) with different carbon black loading (CB): FE-simulation and experimental. Polymer 2012;53(17):3807–14.

[21] Raza MA, Westwood A, Stirling C, Brydson R, Hondow N. Effect of nanosized carbon black on the morphology, transport, and mechanical properties of rubbery epoxy and silicone composites. J Appl Polym Sci 2012;126(2):641–52.

[22] Lu Y, Zhang J, Chang P, Quan Y, Chen Q. Effect of filler on the compression set, compression stress-strain behavior, and mechanical properties of polysulfide sealants. J Appl Polym Sci 2011;120(4):2001–7.

[23] Mallete JG, Quej LM, Marquez A, Manero O. Carbon black-filled PET/HDPE blends: effect of CB structure on rheological and electric properties. J Appl Polym Sci 2001;81(3):562–9.

[24] Shenoy AV. Rheology of filled polymer systems. Norwell: Kluwer Academic Publishers; 1999. p. 248.

[25] Han S, Chung DDL. Mechanical energy dissipation using carbon fiber polymer-matrix structural composites with filler incorporation. J Mater Sci 2012;47:2434–53.

[26] Fu W, Chung DDL. Vibration reduction ability of polymers, particularly polymethylmethacrylate and polytetrafluoroethylene. Polym Polym Compos 2001;9(6):423–6.